Food Chemistry 271 (2019) 650–662

Contents lists available at ScienceDirect

Food Chemistry

journal homepage: www.elsevier.com/locate/foodchem

Characterization of chemical, molecular, thermal and rheological properties of medlar pectin extracted at optimum conditions as determined by Box-Behnken and ANFIS models

Rami H. Al-Amoudi[a], Osman Taylan[a,*], Gozde Kutlu[b], Asli Muslu Can[c], Osman Sagdic[d], Enes Dertli[e], Mustafa Tahsin Yilmaz[a,d,*]

[a] King Abdulaziz University, Faculty of Engineering, Department of Industrial Engineering, P.O. Box 80204, Jeddah 21589, Saudi Arabia
[b] Beykent University, School of Health Sciences, Department of Nutrition and Dietetics, P.O. Box 34522, İstanbul, Turkey
[c] İstanbul Gelişim University, Vocational School, Department of Culinary, P.O. Box 34310, İstanbul, Turkey
[d] Yıldız Technical University, Chemical and Metallurgical Engineering Faculty, Food Engineering Department, P.O. Box 34210, İstanbul, Turkey
[e] Bayburt University, Engineering Faculty, Food Engineering Department, P.O. Box 69000, Bayburt, Turkey

ARTICLE INFO

Keywords:
Medlar fruit
Pectin extraction yield
RSM and ANFIS modeling
Molecular, thermal and rheological characterization

ABSTRACT

In this work, response surface methodology and adaptive neuro-fuzzy inference system approaches were used to predict and model effect of extraction conditions of pectin from medlar fruit (*Mespilus germanica* L.). The pectin extracted at optimized conditions (89 °C, 4.83 h and 4.2 pH) could be classified as high methoxyl pectin. Sugar composition analysis showed that pectin was mainly composed of D-galacturonic acid, L-arabinose, L-rhamnose, D-galactose and D-glucose. Fourier Transform Infrared Spectroscopy, RAMAN and nuclear magnetic resonance spectra confirmed molecular structure, revealing presence of D-galacturonic acid backbone. X-ray diffraction patterns revealed an amorphous structure. Differential scanning calorimetry showed endothermic (123 °C) and exothermic peaks (192 °C). Thermogravimetric analysis revealed three decomposition regions, 50–225 °C, 225–400 °C and 400–600 °C. Steady and dynamic shear analyses revealed that pectin had a pseudo-plastic behavior with storage (G') and loss (G'') modulus increasing with increment in frequency, indicating viscoelastic structure more predominantly elastic than viscous.

1. Introduction

Pectin comprises of backbone of D-galacturonic acid units which were linked by α-1,4 glycosidic linkage located in primary cell and middle part of the land plant (Liu, Cao, Huang, Cai, & Yao, 2010). In the food industry, it is widely used in desserts, dairy products, jams and jellies as well as soft drinks as a gelling, stabilizing and thickening agent (Wang et al., 2016). Moreover, because of its dietary fiber composition and anti-cancer properties, its usage in food as ingredient is of a great importance in terms of health benefits (Zhang, Xu, & Zhang, 2015).

Pectin is not present a free form and should be somehow extracted from natural sources like fruits and vegetables for industrial use. Given that pectin possesses the aforementioned technological and functional properties, the most proper extraction conditions should be applied such that the pectin could be extracted at maximum level with minimum lose in the technological and functional properties since, in the stage of extraction, the structural and physicochemical characteristics of pectin might be remarkably altered depending on methods of extraction. In this respect, several methods have been proposed and tested to increase extraction yield of pectin (Wang et al., 2016).

Fuzzy system offers an opportunity to optimize many process conditions to increase extraction yield. Fuzzy sets and system can be regarded as one of the most important implementations of fuzzy logic and set concept to overcome the variations in multi input single output processes. The fuzzy controllers (if-then rules) are methodically evolved considering the data obtained, rules constitute the backbone of a fuzzy control system. Hence, the ANFIS developed aims to achieve the optimum extraction yield considering the pH, extraction time and temperature on pectin yield of medlar fruit. In this work, on the basis of the first order Sugeno fuzzy approach, an ANFIS model was built up on the training ability of back propagation neural networks (BPNNs) algorithm. The essential asset of a fuzzy sets and system is their assistance to

* Corresponding authors at: Yıldız Technical University, Chemical and Metallurgical Engineering Faculty, Food Engineering Department, P.O. Box 34210, İstanbul, Turkey (M.T. Yilmaz).
E-mail addresses: otaylan@kau.edu.sa (O. Taylan), myilmaz@kau.edu.sa (M.T. Yilmaz).

https://doi.org/10.1016/j.foodchem.2018.07.211
Received 1 June 2018; Received in revised form 30 July 2018; Accepted 30 July 2018
Available online 03 August 2018
0308-8146/

find out the complications resulting from absence of actual-time control and observing of a setback in a production plan in a more comprehensive and most optimal approach. Similarly, experimental design and statistical operation management techniques are a pair of competent implements in optimizing the pectin extraction yield. In literature, several number of investigations have been recently conducted on optimization of the extraction conditions as well as their chemical, thermal and molecular characterization of some novel pectin sources such as okra pods (Alba, Laws, & Kontogiorgos, 2015), grapefruit peel (Wang et al., 2016), tomato waste (Grassino, Halambek et al., 2016; Grassino, Brnčić et al., 2016), nopal (Ibarra-Rodríguez, Lizardi-Mendoza, López-Maldonado, & Oropeza-Guzmán, 2017), okra (Kpodo et al., 2017), Jackfruit peel (Govindaraj, Rajan, Hatamleh, & Munusamy, 2018), citron (Pasandide, Khodaiyan, Mousavi, & Hosseini, 2017), hogweed (Patova et al., 2017) and watermelon rind (Pethowicz, Vriesmann, & Williams, 2017). However, no study has appeared on characterization of pectin extracted from medlar fruit.

Medlar is a genus of *Mespilus germanica* L. which belongs to the *Rosaceae* family. It is cultivated in Turkey as well as in many European countries and Asia and consumed as a fruit. Medlar fruit can be used to produce gellies, sauces and wines. It can be also employed as medicinal purposes for different illnesses primarily for the treatment of constipation and kidney and bladder related diseases. It can be used up as fresh, vinegar, pickle, boiled, pressed and dried fruit pulp (Bostan, 2002). However, the most common utilization is raw consumption. Being a climacteric fruit, it has become more valuable in human consumption, which increases its commercial importance; accordingly, it possess a commercial market in big stores in urban centers and in local outdoor markets. This commercial potential takes attention of researches to reveal its chemical and nutritional properties (Glew et al., 2003a, 2003b).

Legumes and citrus fruits have been reported to have higher amounts of pectin than do cereals, so medlars are among the fruits including high amount of pectin (Alamgir, 2018). As seen, medlar has also been reported (Alamgir, 2018) to be a good source of pectin, which suggests its industrial potential given the wide application areas of pectin in food industry. Therefore, medlar should also be considered as a new source of natural polysaccharides which can be utilized by food industry as a potential functional ingredient for thickening, viscosity enhancing, gelling and texture modifiying purposes.

Some literature survey reveals some studies related to medlar fruit. Fatty acid profile and total antioxidant capacity (Canbey, Atay, & Ogut, 2011), polyphenoloxidase content (Dincer, Colak, Aydin, Kadioglu, & Güner, 2002), sugar, aminoacid and organic acid content (Glew et al., 2003a, 2003b), volatile compounds extracted by supercritical fluid extraction (Pourmortazavi, Ghadiri, & Hajimirsadeghi, 2005), physical and chemical properties (Haciseferogullari, Özcan, Sonmete, & Özbek, 2005), phenolic acid composition and activity of radical scavenge of medlar fruits extracts (Gruz, Ayaz, Torun, & Strnad, 2011) were determined. However, no investigation has been conducted on characterization of pectin extracted from medlar fruit under optimized conditions. Therefore, this study appears to be first attempt to characterize the medlar pectin.

In our study, the relationship between three extraction parameters; i.e. extraction temperature, time and pH along with extraction yield of pectin was modelled using RSM as well as ANFIS method. The process parameters need continuous checking and testing against variations. An optimal range of parameters can be determined to control the optimal extraction yield level of pectin. In order to achieve the optimal extraction yield, empirical, semi-empirical modelling methods, and/or statistical process control approaches can be used. This study; therefore, was undertaken to use Box-Behnken and ANFIS models to optimize effects of extraction parameters; namely, extraction temperature (30–90 °C), time (0.5–5 h) and pH (1.5–6) on pectin extraction yield as well as to characterize medlar pectin extracted at optimized conditions with respect to chemical, molecular, thermal and rheological properties.

2. Materials and methods

2.1. Material and pectin extraction

About 1 kg of wild fresh medlar fruit (*Mespilus germanica* L., wild type, fam: Rosaceae) fruit at maturity was randomly collected from 10-year-old trees, located on the hillsides in İstanbul, Turkey in October, 2016. The fruits were mixed together to produce a homogeneous sample. The fruits were transferred into the laboratory in a nitrogen Dewar flask, and stored deep-frozen until extraction. In this study, the fleshy parts of the fruit without seeds were used as the sample.

The extraction procedure of Kratchanova, Pavlova, and Panchev (2004) was followed with some modifications. The fleshy parts of the fruits were dried at 55 °C for 10 h in drying oven to obtain dry mass. The mass was scoured over a 4 mesh sieve. For extraction, the powder acquired was parted into 15 experimental batches according to the experimental design shown in Table S1 in which the extraction conditions; namely, extraction temperature (30–90 °C), time (0.5–5 h) and pH (1.5–6) were indicated for each batch. Four gram of powder of each batch was mixed with distilled water (1:25) whose pH was adjusted to pH 1.5–6 using 0.1 N HCI and NaOH. The mixture was heated to 30–90 °C for 0.5–5 h using magnetic stirrer, followed by centrifugation at 10.000 rpm for 10 min. The supernatant was collected and added with four volume of ethanol. A cheesecloth was used to collect the precipitated pectin. The collected pectin was dried at 55 °C in drying oven, then ground. The equation below (Eq. (1)) was used to compute yield of extraction (Grassino, Brnčić et al., 2016):

$$EY = \frac{a}{a_0}(w/w) \tag{1}$$

where a and a_0 were amounts of dried pectin mass after extraction and initial amount of dried powder, respectively.

2.2. Experimental design, modeling and optimization

2.2.1. Response surface methodology

In this paper, Box-Behnken design was employed to evaluate effect of factors, namely extraction temperature (X_1), time (X_2) and pH level (X_3) on yield of extraction. Coded and experimental levels of the independent variables are presented in Table S1. The Box-Behnken design was used to fit a three order response surface model with 15 experimental points composed of twelve factorial and three center points. A reduced cubic polynomial equation (Eq. (2)) was acquired by fitting of the experimental data to the three order polynomial equation expanded with appended cubic interaction effects:

$$\begin{aligned} Y\,(\textit{extraction yield}) = {} & \beta_0 + \beta_1 X_1 + \beta_2 X_2 + \beta_3 X_3 + \beta_{12} X_1 X_2 + \beta_{13} X_1 X_3 \\ & + \beta_{23} X_2 X_3 + \beta_{11} X_1^2 + \beta_{22} X_2^2 + \beta_{33} X_3^2 + \beta_{112} X_1^2 X_2 \\ & + \beta_{113} X_1^2 X_3 + \beta_{122} X_1 X_2^2 + \varepsilon \end{aligned} \tag{2}$$

where Y is the predicted response and X_1, X_2, X_3 were the extraction temperature, time X_2 and pH level and ε was the experimental error. The intercept (β_0), the main (β_1, β_2, β_3), interactions (β_{12}, β_{13}, β_{23}, β_{112}, β_{113}, β_{112}) and quadratic (β_{11}, β_{22}, β_{33}) were the regression coefficients.

With an aim to optimize extraction yield, a simultaneous optimization technique used by Karnopp, Oliveira, de Andrade, Postingher, and Granato (2017) was employed. In optimization procedure, desirability functions $d_i(Y_i)$ were employed to acquire the processing conditions, x achieving the "most desirable" response value (extraction yield). These functions can be used according to whether a certain response Y_i will be maximized or minimized.

$$d_i(\hat{y}_i) = \begin{cases} 0 & \hat{y}_i(x) < L_i \\ \left(\frac{\hat{y}_i(x) - L_i}{T_i - L_i}\right)^s & L_i \leqslant \hat{y}_i(x) \leqslant T_i \\ 1 & \hat{y}_i(x) > T_i \end{cases}$$

$$d_i(\hat{y}_i) = \begin{cases} 1 & \hat{y}_i(x) < T_i \\ \left(\frac{\hat{y}_i(x) - U_i}{T_i - U_i}\right)^s & T_i \leqslant \hat{y}_i(x) \leqslant U_i \\ 0 & \hat{y}_i(x) > U_i \end{cases} \quad (3)$$

where L_i, U_i and T_i were lower, upper and target values, respectively, which were desired for response Y_i with L_i, U_i and T_i.

After calculation of each response variable, desirability values were associated with a single desirability index, D. To achieve this, each response was converted to partial desirability function d_i. This dimensionless function was to reverberate the required ranges for each response. Varying between 0 and 1, the range allow to understand least to most desirable, respectively. A weighted geometric mean of n individual desirability functions [Eq. (4)] was computed by employment of global desirability function D (Myers & Montgomery, 1995):

$$D = (d_1^{p1} \times d_2^{p2} \times d_3^{p3} \times \ldots \times d_n^{pi})^{1/\sum p_i} = \left[\prod_{i-1}^{n} d_i^{p_i}\right]^{1/\sum p_i} \quad (4)$$

where p_i is the weighting of the i_{th}, and normalized so that $\sum_{i=1}^{n} p_i = 1$. In the present study, the desired response of "extraction yield" was the maximum of target goal. In order to analyze, model and optimize the experimental data as well as to plot contour and 3D graphs, Design-Expert Software (Stat-Ease Inc.®, Version 7.0 Minneapolis, USA) was employed.

2.2.2. Adaptive neuro-fuzzy inference system

In this work, an ANFIS model was built up by employment of the learning ability of back propagation neural networks (BPNNs) for application of the first order Sugeno fuzzy method. The main goal to use these ANFIS models was to model and optimize the extraction yield of pectin from medlar fruit. The data obtained from experiments were divided into two parts for the training and checking of the BPNN algorithm. This algorithm is an adaptive network in which the nodes perform similar functions (differentiable nonlinear activation functions) on incoming data elements. The input variable membership functions transfer the incoming data elements to an output numerical value. Membership functions (MFs) employed to feature this progression provide fuzzy sets compliance to model using generally employed linguistic variables, such that "the extraction temperature is high" or "the extraction pH is low", "the extraction time is long" and "the extraction yield is poor", etc. In this study, subtractive clustering algorithm was employed to decide the number and type of MFs, and in this application, each data is the element of a set at a rate pointed out by a membership rate. The clustering algorithm is based on an concept to categorize pectin extraction yield as output as fuzzy fractions which coincidence with input parameters data element. In order to minimize the errors of the extraction yield, the back-propagation and the steepest descent algorithms as well as the relevant membership functions are employed. The equation below is used to describe the error function for the p-th sample. Hence 'e' is the error estimator of the neural network.

$$e = \frac{1}{2}\sum_{p=1}^{N} e_p = \frac{1}{2}\sum_{p=1}^{N}\sum_{k=1}^{l} (t_k - o_k)_p^2 \quad (5)$$

where N is the number of data used for training. (t_k) is the pectin extraction yield found by algorithm and (o_k) is the actual extraction yield.

The network was trained with 21 observations that were used to construct model. The checking data set included 90 experimental results and enabled confirmation of the built ANFIS design. ANFIS designs were built up using MATLAB R2014a with Fuzzy Logic Toolbox. The ANFIS design could produce the numerical outcomes related to pectin extraction yield (%). The estimation abilities of the regression and ANFIS designs will be evaluated by a comparison with those of RSM and discussed later.

2.2.3. Accuracy of developed models

The accuracy of the RSM and ANFIS designs was assessed and compared employing certain statistical tools; i.e. coefficient of determination (R^2), mean percentage error (MPE), mean bias error (MBE), root mean square error (RMSE), modelling efficiency (EF) and chi-square (χ^2). It is possible to detect the distinctions between empirical data and model predictions by using the following statistics tools:

$$MPE = \frac{1}{N}\sum_{i=1}^{N} [(\eta_{c_{exp,i}} - \eta_{c_{pre,i}})/\eta_{c_{exp,i}}] \times 100 \quad (6)$$

$$MBE = \frac{1}{N}\sum_{i=1}^{N} (\eta_{c_{pre,i}} - \eta_{c_{exp,i}}) \quad (7)$$

$$RMSE = \left[\frac{1}{N}\sum_{i=1}^{N} (\eta_{c_{exp,i}} - \eta_{c_{pre,i}})^2\right]^{1/2} \quad (8)$$

$$EF = \frac{\sum_{i=1}^{N} (\eta_{c_{exp,i}} - \eta_{c_{exp,ave}})^2 - \sum_{i=1}^{N} (\eta_{c_{pre,i}} \eta_{c_{exp,i}})^2}{\sum_{i=1}^{N} (\eta_{c_{exp,i}} \eta_{c_{exp,ave}})^2} \quad (9)$$

$$\chi^2 = \frac{\sum_{i=1}^{N} (\eta_{c_{exp,i}} \eta_{c_{pre,i}})^2}{N - n_u} \quad (10)$$

where $\eta_{c_{exp,i}}$ was the empirical extraction yield (%), $\eta_{c_{pre,i}}$ was the estimated extraction yield (%), $\eta_{c_{exp,ave}}$ was the mean of empirical extraction yield (%), N is the number of data points and n_u is the number of model parameters.

2.3. Characterization of medlar pectin

The material characterization analyses were conducted on the pectin samples extracted at the optimized levels of extraction conditions (89 °C, 4.83 h and 4.2 pH), resulting in maximum yield (21.58%) calculated by modeling and optimization techniques of RSM and ANFIS, as will be discussed later in detail.

2.3.1. Chemical characterization

Percentage of fat (Soxhelet extractor method), dry matter and ash contents were determined as outlined (AOAC, 1997). The total protein content (5.70 conversion factor) was determined using a nitrogen and protein analyzer. Total carbohydrate content of medlar pectin powder was established according to phenol–sulphuric acid assay (Dubois, Gilles, Hamilton, Rebers, & Smith, 1956). Titrimetric technique was used to establish the degree of esterification (DE), as outlined (Owens et al., 1952). 0.5 g of dried specimen was put into a flask with a volume of 250 mL, wetted and added with 5 mL ethanol and 1 g NaCl. The mixture was solubilized in 100 mL of distilled water free from carbon dioxide. Then, the mixture was stirred continuously to achieve complete dissolution. 0.1 N NaOH was used to titrate the resulting solution with six droplets of phenolphthalein. The amount of consumption (NaOH) was noted as initial titer (V_1, ml). Then, 25 mL of 0.25 M NaOH was added, followed by a vigorous shake and the flask was sealed and enabled to be permanently mixing for 30 min at room temperature to achieve saponification of polymer ester groups. Later, 25 mL of 0.25 M HCl was put and the specimen was agitated till vanishing of pink color. Three droplets of phenolphthalein was put and 0.1 N NaOH was used to titrate the solution until a consistent pink color. The spent volume was noted titer to saponify (V_2, ml). DE was computed employing the below equation:

$$DE(\%) = \frac{V_2}{V_2 + V_1} \times 100 \quad (11)$$

The average molecular weight (M_w) of the pectin samples were estimated using a high performance size exclusion chromatography attached with two columns and a refractive index detector, taking the refractive index increment, *dn/dc* as 0.146 mL/g that is specific for pectin. (BioSep-SEC-S2000 and S4000, Phenomenex Inc., CA, and Agilent 1100 series, CA, USA). A polarimeter (Atago polarimeter, Tokyo, Japan) was used to estimate optical rotation of pectin solution (0.5%, w/v) prepared in distilled water and centrifuged before the estimation.

2.3.2. Polysaccharide composition

The content of monosaccharides; arabinose, rhamnose, galactose, glucose and D-galacturonic acid was determined by HPLC using the method according to DIN 10758 (DIN 10758, 1997) with some modifications. Five g of the extracted pectin was suspended in 25 ml of 1 M methanolic HCl in a flask and the total volume was completed to 70 ml with deionized water. This mixture was stirred at 80 °C for 120 min in a heated magnetic stirrer. After sonicated for 15 min in an ultrasonic bath, the mixture was left to reach 25 °C. The mixture was added with deionized water to achieve a total of 100 ml and further stirred for 2 min in the magnetic stirrer. Then, the mixture was transferred in centrifuge tubes, followed by centrifugation for 10 min at 4500 rpm and filtration. The aqueous layer was filtrated through 0.45 µm membrane and transferred into the HLPC vials. Analysis of monosaccharides was carried out using an HPLC system (Shimadzu LC20A, Japan) equipped with autosampler (Sil20A) and coupled with refractive index detector (RID 20A) and a Zorbax Aclips XDB-C18 column (4.6 mm × 250 mm, 5 µm, Agilent, USA). Each analysis for chemical characterization was replicated two times with three repetitions.

2.3.3. Molecular characterization

2.3.3.1. Characterization by FTIR. The main functional groups of the medlar pectin extracted at the optimum conditions were revealed employing ATR-FTIR (Attenuated Total Reflectance-Fourier Transform Infrared Spectroscopy, a Bruker Tensor 27 spectrometer, Bremen-Germany). The spectra were recorded in the 4000–600 cm^{-1} range with sixteen scans and a resolution of 4 cm^{-1} using a KBr beam splitter and a DLaTGS detector. An ATR accessory supplied with diamond ATR cell was employed along with OPUS program (Version 7.2 for Windows software from Bruker GmbH).

2.3.3.2. Characterization by Raman spectroscopy. Raman spectra of the medlar pectin was acquired using Renishaw Raman microscope system, supplied with an Olympus 20× objective lens. An excitation at 785 nm was achieved by a diode laser to obtain raman spectra. One second of subjection time was implemented by 5% laser power for attaining the Raman spectra in the range of 700–1800 $cm^{-1,}$ which enables enhancement of signal-to-noise ratio of the data.

2.3.3.3. Characterization by nuclear magnetic resonance (^1H NMR and ^{13}C NMR). Samples were solubilized in heavy water (D_2O) to achieve an ultimate concentration of fifteen mg/mL. ^1H NMR and ^{13}C NMR spectra were acquired on a 500.133 MHz and 126.01 MHz, respectively (Bruker Avance III 500 MHz) at 60 °C in D_2O using a 5 mm probe. Digital resolutions in ^1H spectra was 0.15 Hz per point. D_2O was employed as an internal standard at 4.64 ppm to adjust the chemical shifts of ^1H NMR spectra.

2.3.3.4. Characterization of crystalline structure by X-ray diffraction (XRD). XRD analysis was conducted using an X-ray diffractometer (PANalytical X'Pert Pro, Holland). The powder pectin specimen was analyzed by scanning from 5° to 50° diffraction angle (2θ) (step size 0.01° 2θ, time per step: 0.5 s).

2.3.4. Thermal characterization

2.3.4.1. Differential scanning calorimetry (DSC). DSC (Q100, TA Instruments Inc., New Castle, DE, USA) was used to determine the thermal characteristics of medlar pectin. Hermetic aluminum pans were used to cover specimens (five mg) and heated from 25 to 650 °C at a speed of 10 °C/min. For a reference, a blank aluminum pan was used. Nitrogen was the conveying gas employed at a flow rate of 20 ml/min.

2.3.4.2. Thermogravimetric analysis (TGA). A thermogravimetric analyzer (TGA SDT Q600, TA Instruments, New Castle, DE USA) with a regular flow of nitrogen provided at a rate of 20 ml/min was employed to determine thermal stability of five mg of pectin in a temperature range varying between 25 °C and 650 °C at a rate of 10 °C/min. Within the heating range, the weight loss rates due to the thermal decomposition were calculated by a comparison of the original weight with data of weight loss.

2.3.5. Rheological characterization

To evaluate rheological properties of pectin, the pectin solutions at 3, 4.5 and 6% (w/v) were analyzed. The rheological analysis was performed in these pectin solutions. Steady shear analysis was performed by using a strain/stress controlled rheometer (Anton Paar, MRC 302, Austria) under a controlled temperature range provided by a peltier system. A parallel plate configuration (diameter 50 mm, 1.0 mm gap) was used to perform the measurements. One ml of the solution was sheared within the shear rate range of 0.1–100 s^{-1} at a 25 °C. The analysis was replicated three times with two repetitions. Power-law model was employed to fit the collected data employing a Toolmaster™ software (Graz, Austria). The equation below (Eq. (12)) was used to compute consistency coefficient (K) and flow behavior index (n) values to define shear-effected characteristics of the pectin solutions.

$$\sigma = K\dot{\gamma}^n \quad (12)$$

where σ was the shear stress (Pa), K was the consistency coefficient (Pa s^n), $\dot{\gamma}$ was the shear rate (s^{-1}) and n was the flow behavior index (dimensionless).

A temperature sweep test conducted at 0.5 Pa in a range of 5–70 °C was performed to establish temperature dependency of apparent viscosity obtained from steady shear analysis.

Regarding dynamic rheological analysis, the aforementioned parallel plate configuration was employed to perform an amplitude sweep test in strain range of 0.1–100% at 6.283 rad/s in establishment of linear viscoelastic region (LVR). Frequency sweep test was conducted at 0.5% strain within a frequency (ω) range of 0.1–65 rad/s at 25 °C to record storage (G') and loss modulus (G'') values. The cross-over point of G' and G'' was regarded as the gelling or melting temperatures of the pectin solutions, respectively. A non-linear regression was implemented to the curves of G' and G'' data versus ω to calculate largeness of intercepts (K' and K''), slopes (n' and n'') as well as R^2 using following equations:

$$G' = K'(\omega)^{n'} \quad (13)$$

$$G'' = K''(\omega)^{n''} \quad (14)$$

3. Results and discussion

3.1. Modeling and optimization of pectin extraction using RSM

The model could not be sufficiently explained by the full cubic model, thus which was changed by elimination of the insignificant terms by backward elimination regression (BER) procedure whereby non-significant factors and interactions were removed from the models and solely the factors significant at $p < 0.01$, $p < 0.05$ and $p < 0.1$ levels were chosen for building up the reduced model using the BER procedure. The reduced cubic equation for explanation of extraction

yield was given below as an equation (Eq. (15)):

$$Y(\text{extraction yield, } \%) = 5.22 + 3.92X_1 - 0.96X_2 + 0.20X_3 + 0.62X_1X_2 + 3.57X_1X_3 + 0.78X_2X_3 + 3.44X_1^2 + 2.74X_2^2 - 1.33X_3^2 + 5.44X_1^2X_2 + 3.05X_1^2X_3 + 1.15X_1X_2 \quad (15)$$

The third order polynomial equation (Eq. (15)) was used to model and optimize procedures. Accordingly, the cubic model was successfully used in the literature (Sohrabi & Akhlaghian, 2016).

From Table S2 which shows the Box-Behken model statistics and variance analysis, it is clear that the reduced cubic model had the maximum determination of coefficient (R^2), adjusted determination of coefficient (R^2_{adj}), and the lowest standard deviation compared to other models; linear, 2FI and quadratic models. The model is statistically designated as significant based on *F*-value (9497.3) which refers the quite significance of the model. It is desired that lack-of-fit be insignificant, which indicates that the model had a good ability to estimate. All the indicators show that the diminished cubic polynomial model was quite good at exemplifying the operation within the known empirical region (Sohrabi & Akhlaghian, 2016). The coefficient of determination determined to be very close to unity (0.9999) indicates that a definitive correlation was observed between experimental and estimated outputs. The diminished cubic polynomial equation was quite capable of defining the operation at the specified empirical region, which was revealed by high value of the adjusted determination coefficient (R^2_{adj} = 0.999). The measurement distance of the estimated response in relation to its coupled error indicating the proportion of signal to noise describes the adequate precision. It is desirable that the ratio be greater than 4. This was quite lower than the obtained value (336.4) in this study, verifying that the model can be employed to maneuver the design space. Another point which takes an attraction was that the coefficient of variance (C.V.%) was 0.78, a very low value, indicating reliability and repeatability of the design (Sohrabi & Akhlaghian, 2016).

Table S2 also shows that the coefficients of parameter were significant. The ANOVA results indicated linear, interactive and quadratic relations between the effects of factors on extraction yield. The *p*-values lower than 0.05 show that X_1, X_2, X_3, X_1X_2, X_1X_3, X_2X_3, X_1^2, X_2^2, X_3^2, $X_1^2X_2$, $X_1^2X_3$, X_1X_2 were the significant model terms. The significance order of the extraction parameters from the most to the least significant was temperature, time and pH. The highest *F* value (16514.2) and the lowest *p*-value (< 0.0001) was allocated to the temperature among the other variables. From the ANOVA results, it was also clear that all the binary interactions were significant.

Fig. S1 shows the 3D graphs and reflecting contour plots showing way of the extraction variables; temperature, time and pH. The yield of pectin extraction augmented with increment in levels of temperature and time. Regarding the effect of pH, the extraction yield increased, reaching the maximum value at pH 4.2; however, after this point, the extraction yield started to decrease. The possible reasons could be attributed to the fact that the elevated temperature levels lead to soften the plant tissue. Hence, the mass transfer rate could increase in the cell wall. Increase in the temperature levels was also thought to result in breaking of the bonds, giving rise to release of energy at bonds, thus bringing about reaction of dissolving of pectin from the tissues (Maran, 2015). Time was also a remarkable factor increasing the pectin extraction yield. Accordingly, Maran (2015) reported that the pectin needs a time for penetration of the liquid inside and then dissolving in the medium.

In this study, the most desirable (D = 1.000) solution for maximization of yield of pectin extraction corresponds to temperature of 89 °C, time of 4.83 h and 4.21 of pH in order to obtain the extraction yield of 21.58%. This yield value was comparatively higher than those reported in the literature where different pectin sources were extracted. Accordingly, the extraction yields were reported to be 3.6–4.5% w/w pectin from pomace and 3.3–4.4% w/w pectin from gold kiwifruit (Yuliarti, Goh, Matia-Merino, Mavson, & Brennan, 2015), 5.2–12.2% pectin from banana peels (Oliveira et al., 2016) and 8.70–9.30% pectin from waste durian rinds (Maran, 2015). Similar extraction yields were also reported as 15.47–20.44% pectin from navel orange peel (Guo et al., 2012).

3.2. Modeling and optimization of pectin extraction using ANFIS

Theory of fuzzy set ensuring a methodical procedure to answer linguistic knowledge also employs quantitative calculation considering linguistic marks imposed by membership functions. Fuzzy set theory can be employed for process control using fuzzy rule systems, the rules are established by linguistic variables and terms. For instance “the extraction temperature” is a linguistic variable and can be presented by terms such as ‘*low, average, high, very high, and* etc.’ these linguistic variables can be presented by numerical values too. When these variables are represented by linguistic terms, usually a degree of subjectivity and vagueness arises in the judgment of process control. For instance, how high the extraction temperature is? Is it medium, low or etc? Similarly, let us assume that the extraction temperature is 60 °C, what if it is adjusted to 60.5 °C or 63 °C, and how the pectin extraction yield will change? Fuzzy sets and system can answer these kind of questions using the membership functions. The conventional approaches are not able to answer these questions. A new experimental set has to be established and the results have to be observed. These discussions are valid and needs to be clarified. The concept of linguistic variables in fuzzy set is very useful in dealing with situations where the repetitive and expensive experimental sets have to be carried out and also where there are too complicated and poorly described processes that cannot be described understandably by classical mathematical equations.

In this sense, Fig. 1(a) shows the overall system response surface for extraction time and temperature, and Fig. 1(b) shows the surface for pH and time against extraction yield. Fig. 1(c) and (d) show the membership functions of the factors; extraction temperature and time, respectively. These are fine-tuned membership functions used for the linguistic term sets as “*low, average, high*” and “*short, average, long*”, of the input parameters; temperature and time, respectively. From the Fig. 1(a) and (b), it was also observed that there are nonlinear relations between the input parameters and pectin extraction yield. The plots of these parameters showed that the entire output surface of yield of pectin extraction from medlar fruit was highly nonlinear, and the relation of parameters was complex, hence a more elaborate intelligent model must have been employed to carry out further analysis of these problem. In most real life issues, what type of relation would be between the results and the factors is not clearly known. This work presented the implementation of sub-clustering algorithm which allows for decision about what number and type of membership functions would be. In this algorithm, a cluster with a certain degree has each data point, described by a membership level. The output data is categorized to fuzzy parts which corresponds to input factors based on the concept of clustering algorithm. This concept represents the number of rules which would have a fundamental impact on achievement of a good control level. MFs are the constituents of fuzzy rules which shape FIS. In this study, Gaussian MFs (Eqs. (15) and (16)) were used to determine membership degrees. The Gaussian MFs have two parameters; namely, c and σ, where *c* shows the MFs center and *σ* determines the width of MF. Fig. 1(c) and (d) depicts the Gaussian MFs for the two inputs, extraction temperature and time.

$$Gaussian(x, c, \sigma) = e^{-1/2(\frac{x-c}{\sigma})^2} \quad (16)$$

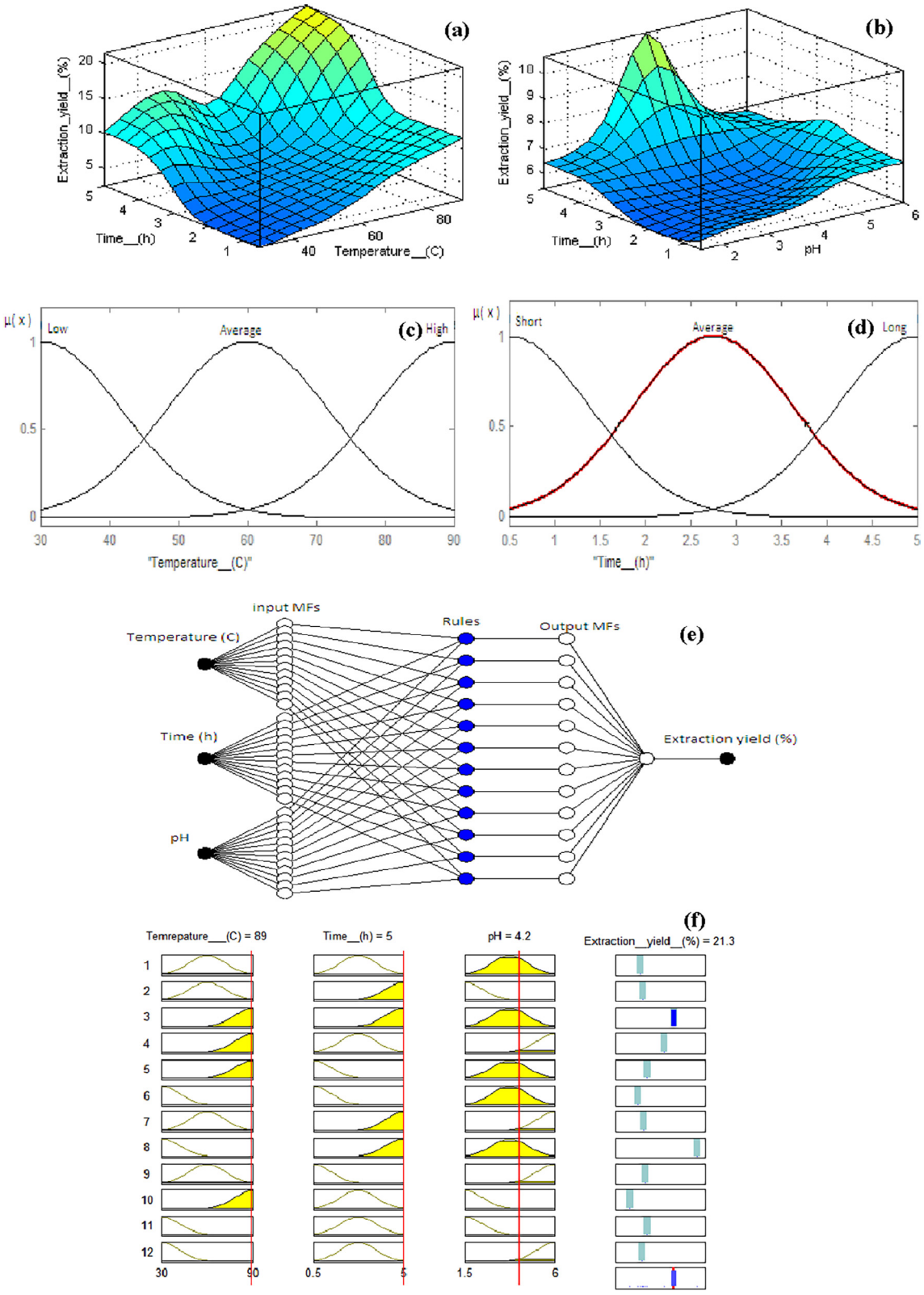

Fig. 1. The overall system response surface for (a) time and temperature, (b) pH and time against extraction yield. (c) and (d) the membership functions of temperature and time, respectively. (e) the ANFIS model architecture and (f) fuzzy reasoning procedures for calculation of the maximum yield of pectin extraction.

$$\mu(Extraction\ \ Temperature) = \mu_{average} = \begin{cases} 0 & for \quad x\langle 30\ and\ x\rangle 90 \\ e^{-1/2\left(\frac{x-60}{15}\right)^2} & for \quad 30 \leqslant x \leqslant 90 \end{cases} \tag{17}$$

In this study, the fuzzy variables were identified by employment of Gaussian membership functions. It is important to establish the number of fuzzy rule in fuzzy sets. Therefore, the quantity of rules equates the quantity of clusters in the concept to subtract cluster. As it was plotted in Fig. 1(e), the fuzzy rules were used in the internal cycle of ANFIS for

Table 1
Chemical characteristics and sugar molar ratios of medlar pectin extracted at optimized conditions.

Chemical properties	
Chemical composition	
Dry matter (%)	8.03 ± 1.58
Ash (%)	4.40 ± 0.04
Protein (%)	0.33 ± 0.03
Fat (%)	–*
Total carbohydrate (%)	87.3 ± 6.5
Physicochemical properties	
Degree of esterification (%)	62.9 ± 1.4
Molar mass (g/mol)	198×10^3
Optical rotation $[\alpha]_D^{20°}$	154°
Saccharide composition (g/100 g)	
D-galacturonic acid (GalA)	71.4 ± 4.85
Neutral sugars	
L-arabinose (Ara)	3.28 ± 0.07
L-rhamnose (Rha)	1.06 ± 0.09
D-galactose (Gal)	7.92 ± 0.16
D-glucose (Glc)	3.72 ± 0.07
ΣSugar†	15.98
Mol% of monosaccharides‡	
Molar ratio of GalA:Ara:Rha:Gal:Glu	79.0:4.09:1.28:10.07:5.01
R1[a]	5.81
R2[a]	0.02
R3[b]	10.57
HG[c]	77.70
RG-I[d]	16.72
HG/RG-I	4.65

* Not detected.
† ΣSugar is the sum of arabinose, rhamnose, galactose and glucose.
‡ Sugar molar ratios (%) of pectins. **R1** = GalA/(Rha + Ara + Gal); **R2** = Rha/GalA; **R3** = (Ara + Gal)/Rha; **HG** (mol%) = GalA (mol%) − Rha (mol%); **RG-I** (mol%) = 2 × Rha (mol%) + Ara (mol%) + Gal (mol%) (Alba et al., 2018).
[a] Linearity.
[b] Degree of branching of RG-I.
[c] Homogalacturonan.
[d] Rhamnogalacturonan.

precise adjustment of the fuzzy model and acquirement of prompt results of pectin extraction rate. The designed ANFIS Architectures was presented in Fig. 1(e) for the extraction yield comprised of three nodes in input layer, 36 nodes ($H_1 \sim H_{36}$) in hidden layer and one node (extraction yield) in the output layer. The neural networks algorithm was trained with the range of influence equaling to 0.56, squash factor equaling to 1.256, accept ratio equaling to 0.56 and reject ratio equaling to 0.15. The sub-clustering algorithm was used to establish quantity of membership functions. It was determined that three membership functions would be sufficient to achieve the optimum extraction yield.

The substantiality of the FIS was augmented by optimization of the learning method by propagation of the error using the BPNNs algorithm. In order to test the training error of various ANFIS designs with various periods, the neural network achieved a targeted training level to acquire method of fuzzy reasoning. The aim of training with different number of MFs was to obtain the lowest error level and obtain maximum yield of pectin extraction. During the training of neural network, the root mean square error (RMSE) of training and checking errors was determined to be 0.1065% and 0.068% for this model, respectively. In this work, an ANFIS model was built up to include sum of 110 fitting parameters which were consisted of 78 non-linear (premise) and 52 linear (resulting) parameters.

The first order Sugeno fuzzy model is shown in Fig. 1(f). Being an approximative reasoning and inference method, the fuzzy reasoning defines the relationships of fuzzy if-then rules and estimate yield of pectin extraction from medlar fruit under different conditions. As it appears in Fig. 1(f), the optimal combination of neuro-fuzzy model were acquired when the quantity of rule is 12. For instance, in this figure, the reasoning procedure clearly shows that the maximum extraction yield would equal to 21.3% if the input parameters; temperature, time and pH equaled to 89 °C, 5 h and 4.2, respectively. In order to achieve this extraction yield, the first rule has been fired. The fuzzy reasoning procedure illustrates that each rule can be fired and crisp outcome of extraction yield can be obtained.

In this study, the investigation depicted that the ANFIS model with 12 rules gave the minimum percentage of error. The average prediction error of models can be calculated using the following equation:

$$\text{The average prediction error } \% = \frac{\sum |\text{Expected value} - \text{Predicted value}|}{\sum \text{Expected value}} \times 100 \quad (18)$$

As a result, the average predicted error of ANFIS model with 12 rules was found to be 0.1867%. Hence, the overall assessment of fuzzy model depicted that the best outcomes could be achieved when the number of rules was 12. On the other hand, the rule optimization appears to be very important for neuro-fuzzy model performance.

3.3. Comparison between RSM and ANFIS

The prediction performance of RSM and ANFIS models were tested by some statistical tools and the calculated constant values which indicate the performance of the models are presented in Table S3. These constants were calculated using the actual values versus predicted values by RSM and ANFIS (Table S1). Table S3 shows that very high values of EF and very low absolute values of MPE, MBE, RMSE and chi-square can be acquired with RSM and ANFIS models. It was also clear from Fig. S2 that both models could adequately describe the relation between experimental (actual) and estimated values (R^2 = 1.000 and 0.9999). Moreover, as was mentioned above, very close levels of extraction variables to maximize the yield of pectin (21.58) were calculated by RSM and ANFIS. These results showed that both RSM and ANFIS can be proposed to model and optimize the pectin extraction yield from medlar fruit.

3.4. Chemical characterization of medlar pectin

The results of analyses used to chemically characterize the pectin extracted from medlar fruit at optimum conditions are presented in Table 1. The dry matter, ash, protein, and carbohydrate contents of the medlar pectin were established to be 8.03%, 4.40%, 0.33% and 87.25%, respectively. No fat was not detected in the medlar pectin. Comparable results were also reported for other pectin sources. Accordingly, total protein level of medlar pectin was lower than those reported for pectin (0.76%) from *Akebia trifoliata* var. *australis* peel (Jiang et al., 2012), pectin (9.4–10.1%) from gold kiwifruit pomace (Yuliarti et al., 2015) and pumpkin pectin (4.58%) (Cui & Chang, 2014). However, dry matter content was slightly higher than that of pectin (7.84%) from *Akebia trifoliata* var. *australis* peel (Jiang et al., 2012), but lower than that of apple pomace pectin (15.93%) (Sharma, Gupto, & Kaushal, 2014), pumpkin pectin (9.6%) (Cui & Chang, 2014). The ash content of the medlar pectin was higher than that of pectin (2.59%) from *Akebia trifoliata* var. *australis* peel (Jiang et al., 2012), that of apple pomace pectin (0.87%) (Sharma et al., 2014), that of gold kiwifruit pectin (3.94%) (Yuliarti et al., 2015) and lower than the value (6.33%) reported for gold kiwifruit pomace pectin (Yuliarti et al., 2015). On the other hand, total carbohydrate content of the medlar pectin was similar to those (ranging between 66 and 87%) of different genotypes of okra pectin (Kpodo et al., 2017) and that (89.3%) of pectin from endocarp of *Citrus depressa* (Tamaki, Konishi, Fukuta, & Tako, 2008). The degree of esterification of medlar pectin was determined to

be 62.9%. This value was greater than 50%, revealing that the medlar pectin belonged to high methoxyl (HM) pectin. On the other hand, the molecular mass of the polysaccharide was estimated to be approximately 198 × 10^3 g/mol. Optical rotation of medlar pectin was determined to be 154°, which reflected the sugar composition.

Table 1 also shows the polysaccharide composition of pectin which accounted for 71.4% D-galacturonic acid, indicating that the polysaccharide included a high amount of galacturonic acid which is the main component of pectin. The molar ratio of D-galacturonic acid, L-arabinose, L-rhamnose, D-galactose and D-glucose was estimated to be 79:4.09:1.28:10.07:5.01, respectively. The mol% values of monosaccharides calculated based on the equations employed by Alba et al. (2018) are also presented in Table 1. The linearity values of pectin were calculated to be 5.81 and 0.02%. The HG/RG-I (ratio of homogalacturonan/rhamnogalacturonan) was calculated as 4.65%, which shows that medlar pectin is of homogalacturonan rich (linear) structure. On the other hand, the monosaccharide composition of medlar pectin was comparable with that of other pectins at different extraction conditions (Tamaki et al., 2008; Wang et al., 2016). The presence of glucose content in medlar pectin may be due to non-pectic polysaccharides such as cellulose and hemicellulose that are adhered to side chains of pectin or residual of solubilizing sugars which could not be entirely taken away in due course of extraction (Wang et al., 2016).

3.5. Molecular characterization of medlar pectin

ATR-FTIR and Raman spectra of medlar pectin are shown in Fig. 2(a) and (b, c, d), respectively. Fig. 2(e) shows theoretical functional group structures of two units of galacturonic acid for pectin acid along with numbering of the atoms (Bichara et al., 2016). In Table 2, the peak designations of vibration bands are given. The most intensive FTIR band at 3286 cm^{-1} was allocated to stretching of O—H bonds while the most intensive Raman band at 2939 was assigned to pyranoid ring carbons (Synytsya, Čopíková, Matějka, & Machovič, 2003). Raman spectra did not reveal the large and intensive O—H stretching band of hydroxyls and bonded water at 3600–3200 cm^{-1} observed in FTIR spectra, which can be attributed to the fact that this stretching band overlaid the infrared C—H stretching band (Synytsya et al., 2003). Raman spectrum had a peak at 1752 cm^{-1} which was assigned to C═O stretching vibration of COOH. This band was not present in the related FTIR spectrum. Medlar pectin had a robust FTIR (1736 cm^{-1}) and a weak Raman (1744 cm^{-1}) bands that were allocated to C═O stretching of COOH. Raman spectrum of medlar pectin had stronger asymmetric carboxylate stretching band (1607 cm^{-1}) than did FTIR spectrum (1610 cm^{-1}) (Fig. 2a and c). This was also case for the symmetric carboxylate stretching bands in both spectrum, revealing the stronger band (1458 cm^{-1}) in Raman spectrum than that (1439 cm^{-1}) in FTIR spectrum. Raman spectrum revealed two bands at 1334 and 1323 cm^{-1} which were allocated to scissoring of C-H groups. These peaks were absent in FTIR spectrum.

Raman analysis allowed interpretation of the total peak area between 800 and 1200 cm^{-1} considered as “a finger print” region which is expressed to be difficult to interpret (Pasandide et al., 2017). Absorptions between 1100 and 1200 cm^{-1} in FTIR spectra were assigned to the R—O—R and cyclic C—C ring referring to glycosidic linkage between sugar units in pectin structure (Liu et al., 2010). The FTIR and Raman spectra also revealed the bands occurring at 1103/1110 cm^{-1} and 1015/1023 cm^{-1}, respectively, which indicated the vibration of C—C and vibration C—O—C of backbone medlar pectin (Liang et al., 2012).

A robust and acute Raman band was seen at 849 cm^{-1} (Table 2) while the corresponding FTIR band was not absent. This was thought to be obscure and overlaid by an intensive absorption at 829 cm^{-1} allocated to out-off-plane vibration of hydroxyls. The frequency of the vibration band at 829–900 cm^{-1} is known to be related to anomeric configuration of carbohydrates (Synytsya et al., 2003). Accordingly, the bands at 829–849 cm^{-1} were assigned to equatorial anomeric H (α-anomers and α-glycosides). Therefore, the Raman band at 849 cm^{-1} was vigorously related to α-glycosidic bonds in medlar pectin (Engelsen & Nørgaard, 1996). The vibration around at 845 cm^{-1} was assigned to C1—H deformation conjoined to a mixed CH_2 vibration after calculation of normal co-ordinate analysis for α-D-glucose (Cael, Koening, & Blackwell, 1973). Based on the reports by Engelsen and Nørgaard (1996) and Synytsya et al. (2003), the Raman band at 849 was assigned to C6—C5—O5—C1—O1 vibration of backbone (Table 2), probably due to sensitivity of the corresponding band of aldopyranoses to the deuteration and oxidation of hydroxyls and C-6 carbon, respectively. The peaks at 682 and 627 cm^{-1} were attributed to vibrations of pyranoid ring at low frequency; in other words, vibrations resulting from skeletal C—C deformation of pectin ring (Grassino, Brnčić et al. (2016)). In the far-infrared range, the shifts revealed by Raman bands with two intensive skeletal shape observed at 436 and 330 cm^{-1} were allocated to the torsion deformation of C—O—C groups (Table 2).

Fig. 2(f) shows the ^{1}H NMR spectrum of medlar pectin. The region including one large singlet at 1.0 ppm was assigned to ethanol (CH_3-CH_2OH) used in pectin extraction to precipitate pectin from the aqueous solution. A sharp and very large singlet at 3.57 ppm was given by the signal from the protons in the methyl group (—OCH_3) united to carboxyl groups (galacturonic acid) (Zhang et al., 2013; Alba et al., 2015; Ibarra-Rodríguez et al., 2017; Govindaraj et al., 2018). The signal at 1.15 and 1.20 ppm was thought to be indicative of the presence of methyl groups of L-rhamnose. The peaks at 2.01 and 1.80 ppm were due to acetyl groups (as depicted in Fig. 2(g)) with 2-O and 3-O galacturonic acid. The signals between 3.6 and 4.6 ppm were attributed to the esterified D-galacturonic acid (Wang et al., 2016). Non-esterified galacturonic acid remnants were revealed by the high proton signals near 5.0 ppm like anomeric H-1 (5.07 ppm) and H-5 (5.01 ppm) (Sharma, Kamboj, Khurana, Singh, & Rana, 2015). Five major signals in Fig. 2 were attributed to the esterified D-galacturonic acid as H-1 protons at 4.72 ppm, H-2 protons at 3.13 ppm, H-3 protons at 3.70 ppm, H-4 protons at 4.32 ppm and H-5 protons at 4.96 ppm (Fig. 2). Therefore, all the ^{1}H NMR signals reveal the presence of D-galacturonic acid in the medlar pectin extracted at optimized conditions.

The ^{13}C NMR spectrum of the extracted medlar pectin is shown in Fig. 2(h). The spectrum shows that there were signals at 54.24 ppm which resulted from the methyl groups (—OCH_3) bound to carboxyl groups of GalA while its corresponding sharp proton singlet was detected at 3.51 ppm in ^{1}H NMR sectra. The signal at 175.86 ppm was assigned to binding of carboxyl groups to methyl groups (Tamaki et al., 2008). The signals at 54.94–63.67 ppm were due to the 3-O methyl galacturonic group (Hokputsa et al., 2004). The peaks at 21.8 ppm was assigned to the O-acetylated residues of GalA structure. In ^{13}C NMR spectra, the signals at 173.6, 73.1, 81.8, 71.2, 65.7 and 99.8 ppm were assigned to C6, C-5, C-4, C-3, C-2 and C-1, respectively anomeric carbons in skeleton of galacturonic ring. ^{1}H NMR and ^{13}C NMR results revealed that the structure of medlar pectin was similar to those of other pectin sources.

Fig. 3 shows pattern of XRD which was conducted to reveal if the medlar pectin would have amorphous or crystalline structure. It was seen that the peaks of medlar pectin at 2θ equals to ~12 and ~21°, which accounts for interatomic distances of 7.1 and 4.2 Å, respectively, putting forward amorphous structure of medlar pectin (Sharma et al., 2015).

3.6. Thermal characterization of medlar pectin

To reveal the thermal behavior of medlar pectin based on the polysaccharide complex, DSC and TGA analyses were conducted. Fig. 3(a) shows the DSC curve which revealed two peaks, i.e. one endothermic peak at 123 °C as melting temperature (T_m) and one exothermic peak as degradation temperature (T_d) at 192 °C, which was in accord with previous studies on pectin (Wang et al., 2016). The T_m

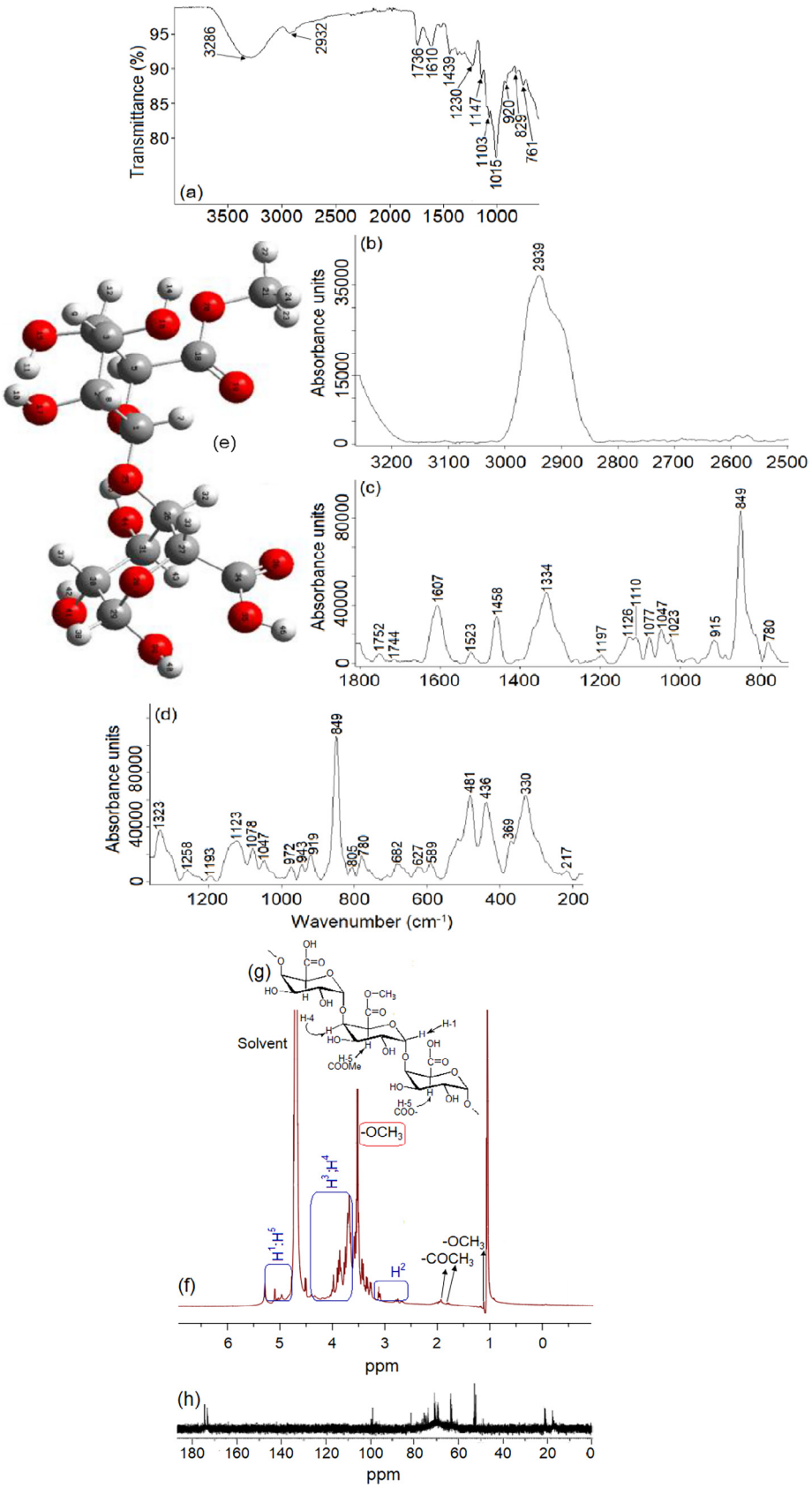

Fig. 2. FT-IR (a) and RAMAN (b, c and d) spectra of medlar pectin extracted at optimized conditions. (e) Theoretical molecular structures of two units of the galacturonic acid for pectin acid together with the atoms numbering (Adapted from Bichara et al., 2016). (f) structure of a fragment of pectin (Adapted from Souza et al., 2012). (g) ^{1}H NMR and (h) ^{13}C NMR spectra.

Table 2
Peak assignments of ATR-FTIR and raman spectrum for medlar pectin extracted at optimized conditions.

Pectin peaks (cm^{-1})			
ATR-FTIR	Raman	Peak assignments [a]	
3286	---	υ(OH)	
2932	2939	υ(CH)	
---	1752	υ(C=O)$_{COOH}$ from methyl esterified carboxyl groups	
1736	1744	υ(C=O)$_{COOH}$ from methyl esterified carboxyl groups	
1610	1607	υ_{as}(COO$^-$)	
1439	1458	υ_{s}(COO$^-$)	
---	1334	δ(CH)	
---	1323	δ(CH)	
1230	1258	δ(OH)$_{COOH}$	
---	1197	υ(COC)$_{glycosidic\ bond,\ ring}$	Finger print
---	1193	υ(COC)$_{glycosidic\ bond,\ ring}$	
1147	1126	υ(COC)$_{glycosidic\ bond,\ ring}$	
---	1123	υ(COC)$_{glycosidic\ bond,\ ring}$	
1103	1110	υ(CC)(CO)	
---	1077	υ(CO) + δ(OH)	
---	1047	υ(CC)(CO)	
1015	1023	υ(CC)(CO)	
---	972	γ(COOH)$_{dimers}$, δ(COO$^-$)	
---	943	δ(CCH), δ(COH)	
920	915	D-glucopyranosyl	
---	849	(C6–C5–O5–C1–O1)	
829	---	γ(C–OH)$_{ring}$, α-D-mannopyranose	
---	805	γ(C–OH)$_{ring}$	
761	780	Ring 'breezing'	
---	682	Low frequency vibrations of pyranoid ring	
---	627	Low frequency vibrations of pyranoid ring	
---	589		
---	481		
---	436	T(C–O–C) def.	
---	369		
---	330	T(C–O–C) def.	
---	217		

[a] ***υ***, stretching; ***δ***, scissoring; γ, wagging or out-of-plane deformation; ***s***, symmetric; ***as***, antisymmetric.

value of medlar pectin was comparatively higher as compared to those informed in literature, suggesting that the medlar pectin had higher DE, galacturonic acid and molecular weight; therefore, more energy was needed to absolutely remove water since endothermic phenomenon is attributed to water evaporation (Einhorn-Stoll, Kunzek, & Dungowski, 2007). The presence of water led to these endothermic peaks which might have also resulted from hydrogen bonds amongst entities of galacturonic acid as well as structural alteration as transforming from stationary $^4C_1$ chair conformation of the galacturonan ring to the inverse $^1C_4$ chair conformation (Einhorn-Stoll & Kunzek, 2009). Based on this report, it can be said that the medlar pectin had high capacity to sustain water based on its high T_m value. On the other hand, the reason why the second peak (T_d) was observed was ascribed to the gradation of pectin due to the heat processing. In other words, the exothermic transition of medlar pectin was observed at 192 °C, revealing that the medlar pectin degraded at this temperature.

Fig. 3(b) shows the TGA curve of medlar pectin, revealing three regions 50–225 °C, 225–400 °C and 400–600 °C, as observed in a previous study (Wang et al., 2016). The first region could be explained based on a small weight loss owing to the vaporization of absorbed water in medlar pectin with an increment in temperature. The second region accounted for a great amount of loss (~45), which was ascribed to the polysaccharide pyrolytic decomposition. This decomposition was

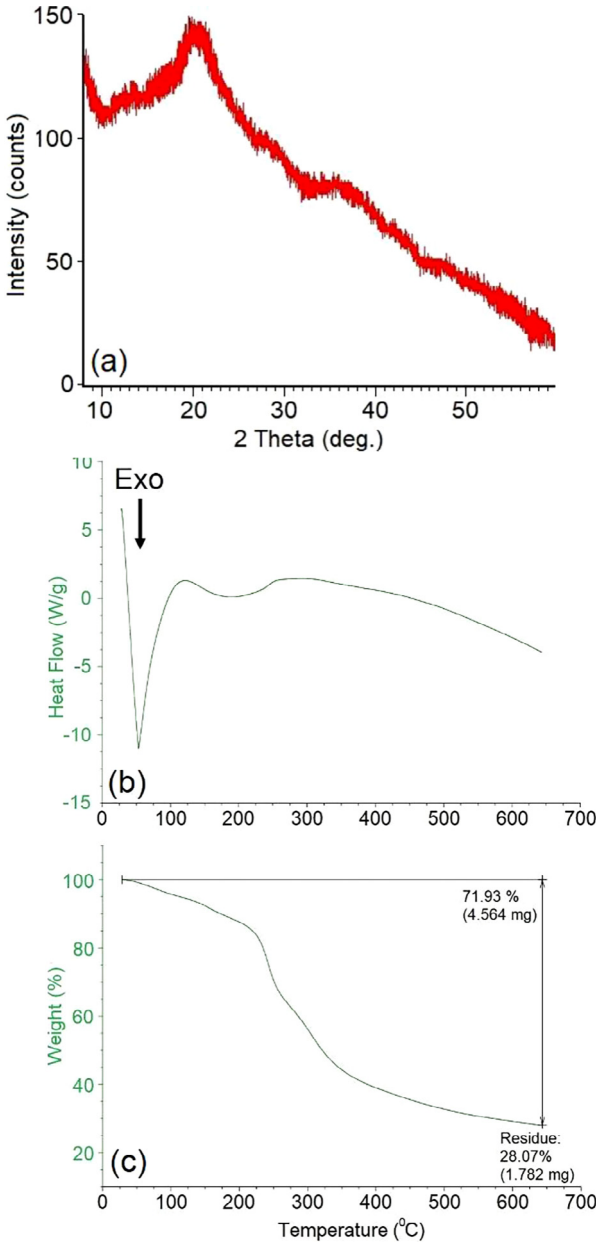

Fig. 3. X-ray powder diffraction pattern (a) and thermal characteristics of medlar pectin extracted at optimized conditions. (b) DSC thermogram and (c) TGA analysis.

explained based on beginning of extensive thermal degradation of galacturonic acid chains, which was followed by formation of decarboxylated acid side group and carbon in the ring resulting in formation of different gaseous products as well as solid char (Wang et al., 2016). In the third region in which the slow mass loss was observed, the char was further thermally decomposed as the pyrolytic temperature increased, giving rise to formation of a partly destroyed and compactly stack solid char containing poly-aromatic structures grafted by aliphatic and ketonic groups (Zhou, Xu, Wang, & Tian, 2011). Accordingly, in the third region, the mass loss of medlar pectin was observed to be around 72%, leaving behind the solid char.

3.7. Rheological characterization of medlar pectin

Fig. 4(a) shows the flow behavior of medlar pectin solutions. The consistency index values presented in Table S4 indicated that the viscosity (consistency coefficient, *K*) of medlar pectin augmented from

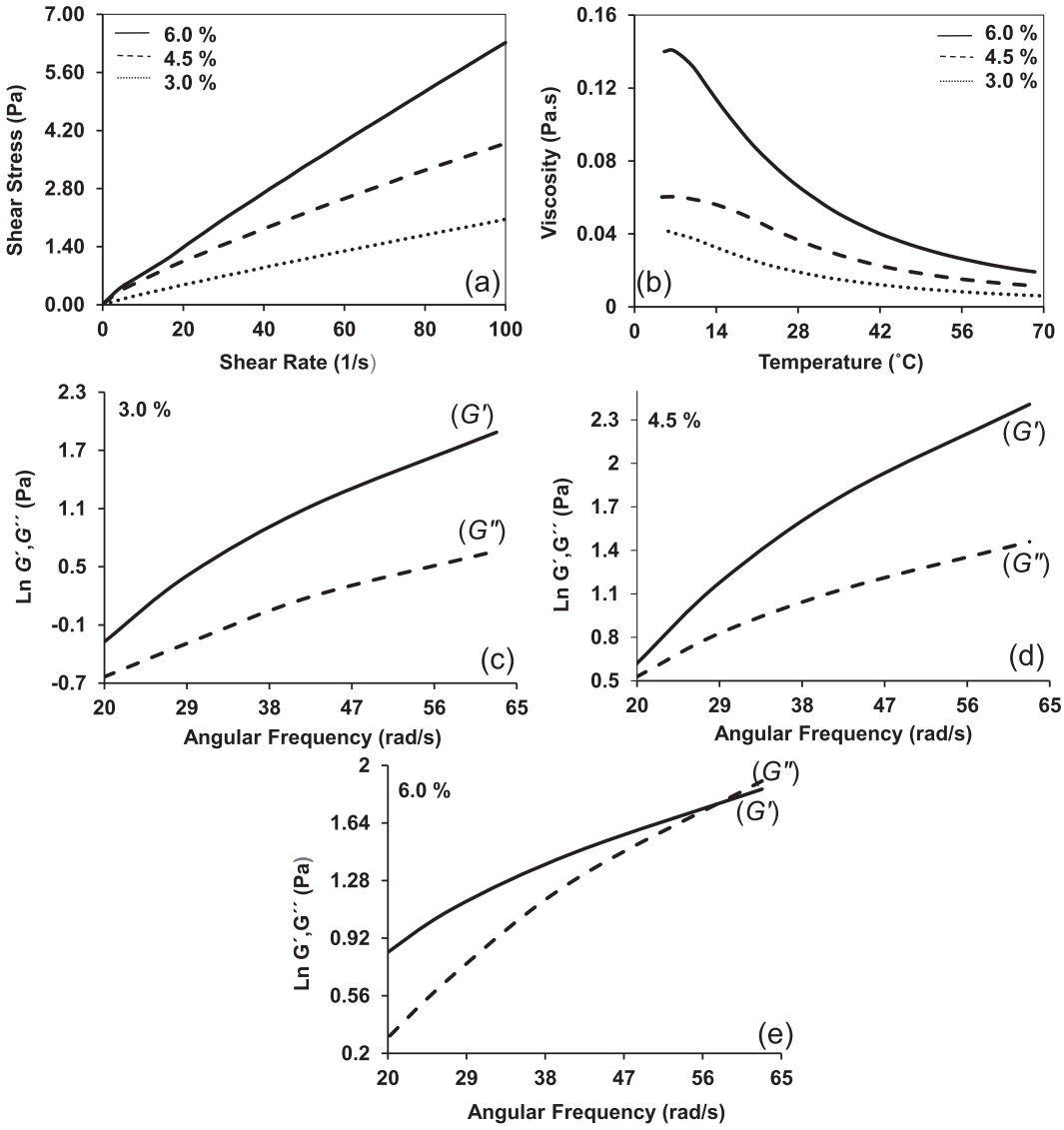

Fig. 4. Steady shear (a) and temperature sweep (b) properties of medlar pectin extracted at optimized conditions. Viscoelastic properties of the pectin at different concentrations, 3.0, 4.5 and 6.0% (c, d and e, respectively).

0.035 to 0.104 Pa s^n with an increment in the concentration of solutions. Higher viscosity values were observed by Wang et al. (2016) who revealed that the viscosity of grapefruit peel pectin solutions at 1, 2 and 3% increased from 0.011 to 0.612 Pa s^n with increase in concentration. Pasandide et al. (2017) reported that the viscosity of citrus medica peel changed from 0.004 to 0.015 Pa s^n as the pectin concentration increased from 0.1 to 2%, revealing the smaller viscosity values as compared to those reported for medlar pectin.

From Fig. 4(a), it is also clear that the shear stress values augmented with an increase in shear rate, indicating that the pectin solutions had non-Newtonian pseudoplastic behavior (shear-thinning). It is generally explained that the pseudoplastic behavior is due to disentanglement of the polymer network and the partial chain orientation in the shear flow direction (Kumbar, Nedomova, Pytel, Kilian, & Buchar, 2017). After a further increase point, the interactions between the molecules may be diminished owing to a micro-structural anisotrophy arising from shear deformation, thus which lowers the viscosity to a nearly invariant value (Jun, Il Lee, Song, & Kim, 2006). Shear-thinning behavior was also confirmed with flow behavior index values which were lower than 1, as presented in Table S4. Wang et al. (2016) reported the counterpart attitude. In addition, the temperature sweep test was performed to understand thermal behavior of pectin solutions in different temperature levels. Fig. 4(b) presents temperature sweep properties of pectin solutions, showing that the viscosity decreased as the temperature level increased up to 70 ˚C. The decrease in the viscosity was more remarkable in pectin solution at 6%.

Viscoelastic characteristics of the solutions were evaluated by the frequency sweep measurements, showing that the modulus (G' and G'') of the pectin solutions augmented with an increment in angular frequency (Fig. 4 c, d and e). The mechanical response predominantly acted like a gel, with G' higher than G'' over the frequency range. The power low parameters of G' and G'' for all the concentrations are given in Table S4. The results showed that both K' and K'' values ascended with augmenting concentration levels, indicating that the viscoelastic nature was more prevalent with increasing pectin concentration. On the other hand, the K' values were calculated to be higher than K'', showing that the pectin solutions were predominantly elastic than viscous. Similar behaviors were reported for citrus pectins; namely grapefruit peel pectin (Wang et al., 2016). It should be also noted here that Fig. 4(e) shows a cross-over point at 58 rad/s indicating viscoelastic behavior of medlar pectin. It typically behaves like a gel with $G' > G''$ until 58 rad/s, and as a liquid with $G'' > G'$ after 58 rad/s, defining a sol–gel attitude and moduli which was comparatively dependent on frequency.

4. Conclusions

In this study, the material characterization analyses were conducted on the medlar pectin extracted at the extraction conditions; i.e. 89 °C, 4.83 h and 4.2 pH, resulting in maximum pectin yield (21.58%) calculated by Box-Behnken and ANFIS modeling. Both model gave excellent results which confirms each other. Extraction conditions are of a great importance because they would have a direct effect on the chemical properties of pectin extracted from pectin. Chemical and molecular analyses like FTIR, Raman, ^{1}H NMR and XRD techniques were also carried out to reveal the molecular structure of medlar pectin. Thermal and rheological behavior of the medlar pectin was also determined. In conclusion, these results revealed the chemical, molecular, thermal and rheological properties of medlar pectin, providing a basic knowledge for future efforts to commercialize medlar pectin in food industry as a commercial hydrocolloid.

Acknowledgements

Special thanks should go to Prof. Dr. Sezgin BAKIRDERE in Chemistry Department of Yıldız Technical University regarding his contributions to conduct characterization analyses.

Appendix A. Supplementary material

Supplementary data associated with this article can be found, in the online version, at https://doi.org/10.1016/j.foodchem.2018.07.211.

References

Alamgir, A. N. M. (2018). *Therapeutic use of medicinal plants and their extracts.* Springer826.

Alba, K., Laws, A. P., & Kontogiorgos, V. (2015). Isolation and characterization of acetylated LM-pectins extracted from okra pods. *Food Hydrocolloids, 43*, 726–735.

Alba, K., MacNaughtan, W., Laws, A. P., Foster, T. J., Campbell, G. M., & Kontogiorgos, V. (2018). Fractionation and characterization of dietary fibre from blackcurrant pomace. *Food Hydrocolloids, 81*, 398–408.

AOAC (1997). Association of Official Analytical Chemists.Official Methods of Analysis. 20th ed., Washington.

Bichara, L. C., Alvarez, P. E., Bimbi, M. V. F., Vaca, H., Gervasi, C., & Brandan, S. A. (2016). Structural and spectroscopic study of a pectin isolated from citrus peel by using FTIR and FT-Raman spectra and DFT calculations. *Infrared Physics & Technology, 76*, 315–327.

Bostan, S. Z. (2002). Interrelations among pomological traits and selection of medlar (*Mespilus Germanica* L.) types in Turkey. *Journal American Pomological Society, 56*(4), 215–218.

Cael, J. J., Koening, J. L., & Blackwell, J. (1973). Infrared and Raman spectroscopy of carbohydrates. Part 3. Raman spectra of the polymorphic forms of amylose. *Carbohydrate Research, 29*, 123–134.

Canbey, H. L., Atay, E., & Ogut, S. (2011). Determination of fruit characteristics, fatty acid profile and total antioxidant capacity of Istanbul Medlar Variety (*Mespilus germanica* L.). *Current Opinion in Biotechnology, 22*, 142.

Cui, S. W., & Chang, Y. H. (2014). Emulsifying and structural properties of pectin enzymatically extracted from pumpkin. *LWT – Food Science and Technology, 58*, 396–403.

DIN 10758. (1997) Analysis of honey-determination of the content of saccharides fructose, glucose, saccharose, turanose and maltose-HPLC method.

Dincer, B., Colak, A., Aydin, N., Kadioglu, A., & Güner, S. (2002). Characterization of polyphenoloxidase from medlar fruits (*Mespilus germanica* L., Rosaceae). *Food Chemistry, 77*, 1–7.

Dubois, M., Gilles, K. A., Hamilton, J. K., Rebers, P. A., & Smith, F. (1956). Colorimetric method for determination of sugars and related substances. *Analytical Chemistry, 28*, 350–356.

Einhorn-Stoll, U., Kunzek, H., & Dungowski, G. (2007). Thermal analysis of chemically and mechanically modified pectins. *Food Hydrocolloids, 21*(7), 1101–1112.

Einhorn-Stoll, U., & Kunzek, H. (2009). Thermoanalytical characterisation of processing-dependent structural changes and state transitions of citrus pectin. *Food Hydrocolloids, 23*(1), 40–52.

Engelsen, S. B., & Nørgaard, L. (1996). Comparative vibrational spectroscopy for determination of quality parameters in amidated pectins as evaluated by chemometrics. *Carbohydrate Polymers, 30*(1), 9–24.

Glew, R. H., Ayaz, F. A., Sanz, C., VanderJagt, D. J., Huang, H. S., Chuang, L. T., et al. (2003). Changes in sugars, organic acids and amino acids in medlar (*Mespilus germanica* L.) during fruit development and maturation. *Food Chemistry, 83*, 363–369.

Glew, R. H., Ayaz, F. A., Sanz, C., VanderJagt, D. J., Huang, H. S., Chuang, L. T., et al. (2003). Effect of postharvest period on sugars, organic acids and fatty acids composition in commercially sold medlar (*Mespilus germanica* 'Dutch') fruit. *European Food Research and Technology, 216*, 390–394.

Govindaraj, D., Rajan, M., Hatamleh, A. A., & Munusamy, M. A. (2018). From waste to high-value product: Jackfruit peel derived pectin/apatite bionanocomposites for bone healing applications. *International Journal of Biological Macromolecules, 106*, 293–301.

Grassino, A. N., Halambek, J., Djakovic, S., Brncic, S. R., Dent, M., & Grabaric, Z. (2016). Utilization of tomato peel waste from canning factory as a potential source for pectin production and application as tin corrosion inhibitor. *Food Hydrocolloids, 52*, 265–274.

Grassino, A. N., Brnčić, M., Vikić-Topić, D., Roca, S., Dent, M., & Brnčić, S. R. (2016). Ultrasound assisted extraction and characterization of pectin from tomato waste. *Food Chemistry, 198*, 93–100.

Gruz, J., Ayaz, F. A., Torun, H., & Strnad, M. (2011). Phenolic acid content and radical scavenging activity of extracts from medlar (*Mespilus germanica* L.) fruit at different stages of ripening. *Food Chemistry, 124*, 271–277.

Guo, X., Han, D., Xi, H., Rao, L., Liao, X., Hu, X., et al. (2012). Extraction of pectin from navel orange peel assisted by ultra-high pressure, microwave or traditional heating: A comparison. *Carbohydrate Polymers, 88*, 441–448.

Haciseferogullari, H., Özcan, M., Sonmete, M. H., & Özbek, O. (2005). Some physical and chemical parameters of wild medlar (*Mespilus germanica* L.) fruit grown in Turkey. *Journal of Food Engineering, 69*, 1–7.

Hokputsa, S., Harding, S. A., Inngjerdingen, K., Jumel, K., Michaelsen, T. E., Heinze, T., et al. (2004). Bioactive polysaccharides from the stems of the Thai medicinal plant Acanthus ebracteatus: Their chemical and physical features. *Carbohydrate Research, 339*, 753–762.

Ibarra-Rodríguez, D., Lizardi-Mendoza, J., López-Maldonado, E. A., & Oropeza-Guzmán, M. T. (2017). Capacity of 'nopal' pectin as a dual coagulant-flocculant agent for heavy metal removal. *Chemical Engineering Journal, 323*, 19–28.

Jiang, Y., Yanxue, D., Zhu, X., Xiong, H., Woo, M. W., & Hu, J. (2012). Physicochemical and comparative properties of pectins extracted from *Akebia trifoliata* var. *australis* peel. *Carbohydrate Polymers, 87*, 1663–1669.

Jun, H., Il Lee, C. H., Song, G. S., & Kim, Y. S. (2006). Characterization of the pectic polysaccharides from pumpkin peel. *LWT – Food Science and Technology, 39*(5), 554–561.

Karnopp, A. R., Oliveira, K. G., de Andrade, E. F., Postingher, B. M., & Granato, D. (2017). Optimization of an organic yogurt based on sensorial, nutritional, and functional perspectives. *Food Chemistry, 233*, 401–411.

Kpodo, F. M., Agbenorhevi, J. K., Alba, K., Bingham, R. J., Oduro, I. N., Morris, G. A., et al. (2017). Pectin isolation and characterization from six okra genotypes. *Food Hydrocolloids, 72*, 323–330.

Kratchanova, M., Pavlova, E., & Panchev, I. (2004). The effect of microwave heating of fresh orange peels on the fruit tissue and quality of extracted pectin. *Carbohydrate Polymers, 56*, 181–185.

Kumbar, V., Nedomova, S., Pytel, R., Kilian, L., & Buchar, J. (2017). Study of rheology and friction factor of natural food hydrocolloid gels. *Potravinarstvo Slovak Journal of Food Sciences, 11*(1), 203–209.

Liang, R., Chen, J., Liu, W., Liu Cm, Y. W., Yuan, M., & Xq, Z. (2012). Extraction, characterization and spontaneous gel-forming property of pectin from creeping fig (*Ficus pumila* Linn.) seeds. *Carbohydrate Polymers, 87*, 76–83.

Liu, L., Cao, J., Huang, J., Cai, Y., & Yao, J. (2010). Extraction of pectins with different degrees of esterification from mulberry branch bark. *Biosource Technology, 101*, 3268–3273.

Maran, J. P. (2015). Statistical optimization of aqueous extraction of pectin from waste durian rinds. *International Journal of Biological Macromolecules, 73*, 92–98.

Myers, R. H., & Montgomery, D. C. (1995). *Response Surface Methodology. Process and Product Optimization Using Designed Experiments.* New York, USA: Wiley705.

Oliveira, T.İ. S., Rosa, M. F., Cavalcante, F. M., Pereira, P. H. F., Moates, G. K., Wellner, N., et al. (2016). Optimization of pectin extraction from banana peels with citric acid by using response surface methodology. *Food Chemistry, 198*, 113–118.

Owens, H. S., McCready, R. M., Shepherd, A. D., Schultz, S. H., Pippen, E. L., Swenson, H. A., et al. (1952). *Methods used at western regional research laboratory for extraction and analysis of pectic materials. AIC-340.* Western: Regional Research Laboratory, Albany, California.

Pasandide, B., Khodaiyan, F., Mousavi, Z. E., & Hosseini, S. S. (2017). Optimization of aqueous pectin extraction from *Citrus medica* peel. *Carbohydrate Polymers, 178*, 27–33.

Patova, O. A., Golovchenko, V. V., Vityazev, F. V., Burkov, A. A., Belyi, V. A., Kuznetsov, S. N., et al. (2017). Physicochemical and rheological properties of gelling pectin from Sosnowskyi's hogweed (*Heracleum sosnowskyi*) obtained using different pretreatment conditions. *Food Hydrocolloids, 65*, 77–86.

Pethowicz, C. L. O., Vriesmann, L. C., & Williams, P. A. (2017). Pectins from food waste: Extraction, characterization and properties of watermelon rind pectin. *Food Hydrocolloids, 65*, 57–67.

Pourmortazavi, S. M., Ghadiri, M., & Hajimirsadeghi, S. S. (2005). Supercritical fluid extraction of volatile components from *Bunium persicum* Boiss. (black cumin) and *Mespilus germanica* L. (medlar) seeds. *Journal of Food Composition and Analysis, 18*, 439–446.

Sharma, P. C., Gupto, A., & Kaushal, P. (2014). Optimization of method for extraction of pectin from apple pomace. *Indian Journal of Natural Products and Resources, 5*, 184–189.

Sharma, R., Kamboj, S., Khurana, R., Singh, G., & Rana, V. (2015). Physicochemical and functional performance of pectin extracted by QbD approach from *Tamarindus indica* L. *Carbohydrate Polymers, 134*, 364–374.

Sohrabi, S., & Akhlaghian, F. (2016). Modeling and optimization of phenol degradation over copper-doped titanium dioxide photocatalyst using response surface

methodology. *Process Safety and Environmental Protection, 99*, 120–128.
Souza, J.R.R., Feitosa, J.P.A., Ricardo, N.M.P.S., & Brito, E.S. (2012). Isolation and Characterization of Pumpkin Pectin for Drug Encapsulation. COLAOB, Congresso Latino Americano de Órgãos Artificiais Biomateriais. 22–25 August 2012, Natal, RN.
Synytsya, A., Čopíková, J., Matějka, P., & Machovič, V. (2003). Fourier transform Raman and infrared spectroscopy of pectins. *Carbohydrate Polymers, 54*, 97–106.
Tamaki, Y., Konishi, T., Fukuta, M., & Tako, M. (2008). Isolation and structural characterization of pectin from endocarp of *Citrus depressa*. *Food Chemistry, 107*, 352–361.
Wang, W., Ma, X., Jiang, P., Hu, L., Zhi, Z., Chen, et al. (2016). Characterization of pectin from grapefruit peel: A comparison of ultrasound-assisted and conventional heating extractions. *Food Hydrocolloids, 61*, 730–739.
Yuliarti, O., Goh, K. K. T., Matia-Merino, L., Mavson, J., & Brennan, C. (2015). Extraction and characterisation of pomace pectin from gold kiwifruit (*Actinidia chinensis*). *Food Chemistry, 187*, 290–296.
Zhang, L., Ye, X., Ding, T., Sun, X., Xu, Y., & Liu, D. (2013). Ultrasound effects on the degradation kinetics, structure and rheological properties of apple pectin. *Ultrasonic Sonochemistry, 20*, 222–231.
Zhang, W., Xu, P., & Zhang, H. (2015). Pectin in cancer therapy: A review. *Trends in Food Science & Technology, 44*, 258–271.
Zhou, S., Xu, Y. B., Wang, C. H., & Tian, Z. F. (2011). Pyrolysis behavior of pectin under the conditions that simulate cigarette smoking. *Journal of Analytical and Applied Pyrolysis, 91*(1), 232–240.